Original Article

Quantitative analysis of sagittal curvatures of the tibial plafond by computed tomography

Yuanjun Teng[1,2,3], Hu Luo[1], Yifan Cai[3], Sixian Li[4], Jian Yu[2], Kangrui Zhang[3], Fan Lu[3], Wenming Chen[1], Xu Wang[2], Xin Ma[1,2,5]

[1]Academy for Engineering and Technology, Fudan University, Shanghai, China; [2]Department of Orthopedic Surgery, Huashan Hospital, Fudan University, Shanghai, China; [3]Department of Orthopedics, Lanzhou University Second Hospital, Lanzhou University, Lanzhou, China; [4]Medical College, Yangzhou University, Yangzhou, China; [5]Department of Orthopedics, Shanghai Sixth People's Hospital Affiliated to Shanghai Jiao Tong University School of Medicine, Shanghai, China

Contributions: (I) Conception and design: Y Teng, J Yu, X Ma; (II) Administrative support: All authors; (III) Provision of study materials or patients: Y Teng, H Luo, Y Cai, S Li, F Lu, W Chen; (IV) Collection and assembly of data: Y Teng, H Luo, Y Cai, S Li, J Yu, K Zhang, X Wang; (V) Data analysis and interpretation: All authors; (VI) Manuscript writing: All authors; (VII) Final approval of manuscript: All authors.

Correspondence to: Xin Ma, MD, PhD. Academy for Engineering and Technology, Fudan University, No. 220 Handan Rd., Yangpu District, Shanghai 200433, China; Department of Orthopedic Surgery, Huashan Hospital, Fudan University, Shanghai, China; Department of Orthopedics, Shanghai Sixth People's Hospital Affiliated to Shanghai Jiao Tong University School of Medicine, Shanghai, China. Email: maxinprof@126.com.

Background: Although the talar morphology has been well understood, studies on the corresponding tibial plafond are still lacking. Based on computed tomography (CT) data, this quantitative study divided the tibial plafond into anterior and posterior regions on five sagittal sections. The objectives of this study were (I) to determine whether the sagittal curvatures of the tibial plafond can be quantitatively and accurately described using the double-diameter method; (II) to compare the difference between the anterior and posterior diameters on five sagittal sections.

Methods: In this study, CT data were collected from 100 adult ankles, and the three-dimensional (3D) ankle joint model was reconstructed using CT images. An anatomical coordinate system of the 3D ankle joint model was created to establish the standard coronal and sagittal planes. The measurement outcomes of sagittal curvatures included: the anterior and posterior diameters, the distal tibial arc length (TiAL) and the distal tibial mortise depth (TMD) on five sagittal sections (the most medial, medial 1/4, middle, lateral 1/4 and the most lateral section). Subgroup analysis was performed to compare the differences between males and females.

Results: Analysis of the sagittal curvatures showed that the anterior diameter of tibial plafond was significantly smaller than the posterior diameter on five sagittal sections with a mean difference ranging from 3.9 to 6.8 mm ($P<0.001$). For the anterior diameters, the anteromedial curve had the smallest diameter (35.3±5.3 mm), and the anterolateral curve had the largest diameter (38.0±5.8 mm). For the posterior diameter, the posteromedial curve had the smallest diameter (39.2±6.4 mm), and the posterolateral 1/4 curve had the largest diameter (43.5±6.9 mm). One-way analysis of variance (ANOVA) revealed significant differences in the anterior and posterior diameters among five groups ($P<0.012$). Subgroup analysis showed that gender partly affected the results of sagittal curvature measurements.

Conclusions: The sagittal curvatures of the tibial plafond can be described quantitatively and accurately using anterior and posterior diameters. Our study showed that there were significant differences between the anterior and posterior diameters, and gender was an important factor influencing the sagittal curvatures of the tibial plafond.

Keywords: Tibial plafond; sagittal curvature; ankle joint; computed tomography (CT); quantitative analysis

Submitted Dec 20, 2023. Accepted for publication May 20, 2024. Published online Jun 07, 2024.
doi: 10.21037/qims-23-1807
View this article at: https://dx.doi.org/10.21037/qims-23-1807

Introduction

The ankle joint produces six degrees of freedom of motion as a result of a complex interaction of ligamentous constraints, bony and articular surfaces, and other adjacent joints (1). However, the fundamental properties of the ankle kinematics and biomechanics are mainly determined by the anatomical morphology of the talus and tibial plafond (2,3). To date, the detailed anatomical characteristics of the ankle joint still need further studied.

In recent decades, considerable attention has been paid to the sagittal geometry of the talus. Previous studies (1,4) usually used a single-radius curve to describe the sagittal geometry of the talar dome, and found that the medial radius of the talar dome was significantly larger than the lateral radius. More recently, Nozaki *et al.* (5) utilized a bi-radial approach to evaluate the anterior and posterior radii of the talar trochlea in fifty dry tali from Asian populations. They showed that the shape of the talus was bilaterally asymmetric, resulting in opposite axial rotations during ankle plantarflexion and dorsiflexion. Although the talar morphology has been well understood, studies of the corresponding tibial plafond are still lacking.

Inman *et al.* (6) firstly assessed the anatomical curvatures of the distal tibia using saw cuts to obtain the sagittal plane on cadaveric bones. Subsequently, Wiewiorski *et al.* (7) utilized a single-radius method to evaluate the morphologic changes of the tibial plafond in patients with end-stage ankle osteoarthritis. In addition, numerous studies have examined only the talar morphology without analyzing the corresponding tibial morphology (1,5,8,9). Clinically, a detailed and accurate description of sagittal parameters in the radii, distal tibial arc length (TiAL) and the distal tibial mortise depth (TMD) at the tibial plafond contributes to optimize the fracture treatment, deformity correction and implant design (2,5). Moreover, data on morphological gender differences serve as critical references for the design and sizing of gender-specific prosthesis between males and females. However, few studies have measured the sagittal curvatures of the tibial plafond using the double-diameter method and compared the anatomical differences in different genders. Therefore, we designed this study to quantitatively evaluate the anatomical morphology of the tibial plafond based on computed tomography (CT) images.

In this study, we divided the tibial plafond into anterior and posterior regions on five sagittal sections. The objectives of the present study were (I) to determine whether the sagittal curvatures of the tibial plafond can be quantitatively and accurately described using the double-diameter method; (II) to compare the difference between the anterior and posterior diameters on five sagittal sections. We present this article in accordance with the STROBE reporting checklist (available at https://qims.amegroups.com/article/view/10.21037/qims-23-1807/rc).

Methods

The study was conducted in accordance with the Declaration of Helsinki (as revised in 2013). The Ethics Committee of Lanzhou University Second Hospital approved this study (No. 2022A-556), and the requirement to obtain individual consent for this retrospective analysis was waived.

Subject selection

This study was a retrospective study based on CT images. The protocol has been approved by our institutional review board. CT data between January 2018 and December 2022 were obtained from our healthy ankle CT database. All skeletally mature subjects with age from 18 to 60 years were eligible for study participation. Individuals with a history of ankle fracture, degenerative joint disease, tumor and deformity around the ankle, and any surgery around the ankle were excluded.

CT Imaging and three-dimensional (3D) bone model reconstruction

Routine ankle CT scans were performed with a 64-detector-row CT scanner (Siemens AG, Germany) in the supine position. CT acquisition parameters included a gantry rotation speed of 1.00 s/rotation, a CT pitch factor of 0.90, a slice thickness of 0.625 mm, and a field of view of 25 to 30 cm. CT images were imported into Mimics software (version 21.0, Materialise, Leuven, Belgium) to reconstruct 3D bone

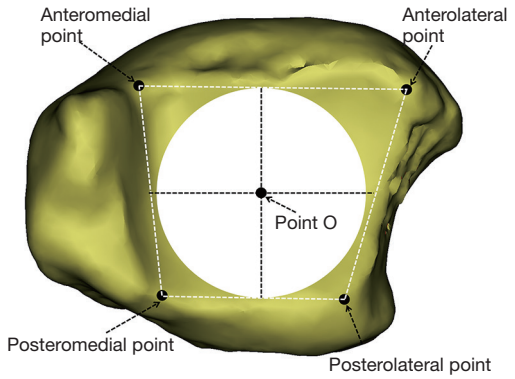

Figure 1 Establishment of the origin of the coordinate system (Point O). The origin was defined as the center of the tibial plafond. The method of best-fit circle was used to determine the center of the tibial plafond using the anteromedial, posteromedial, anterolateral, and posterolateral points.

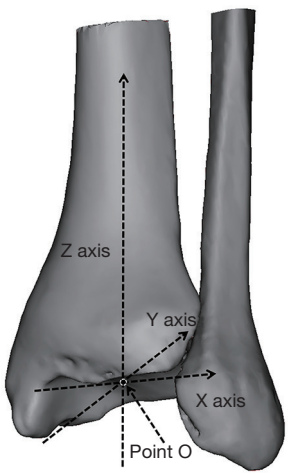

Figure 2 Establishment of the ankle coordinate system.

models of the ankle joint. All the models were reconstructed by an experienced orthopedic surgeon (Y.T.).

Ankle coordinate system

To obtain standard coronal and sagittal ankle planes, an ankle coordinate system was established as described in previous studies (10-12). First, the origin (Point O) of the coordinate system was defined as the tibial plafond center (*Figure 1*). Second, the medial-lateral axis of the tibia was defined as the line passing Point O and parallel to the line connecting anteromedial and anterolateral points of the tibial plafond (12). The superior-inferior axis was defined as

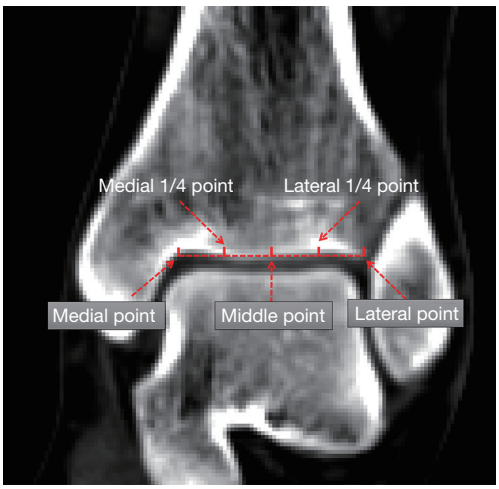

Figure 3 Quantitatively dividing the tibial plafond. The tibial plafond was divided equally into four segments by five points (medial point, medial 1/4 point, midpoint, lateral 1/4 point, lateral point).

the line connecting Point O and midpoints of outer cortical diameter at 10 cm proximal to the ankle joint. The coronal plane was established using the medial-lateral and superior-inferior axes. The sagittal plane was defined as a plane perpendicular to the coronal plane. The transverse plane was defined as a plane perpendicular to both the coronal and sagittal planes. After establishing the anatomical coordinate system, we used the resliced technique of 3D-CT images to generate the standard coronal and sagittal planes. All the measurements were performed with respect to this coordinate system (*Figure 2*).

Sagittal curvature measurements of the tibial plafond

Based on the standard coronal and sagittal planes, the anterior and posterior diameters of the tibial plafond in ten regions were calculated according to the procedure reported in previous studies (13,14). First, to quantitatively divide the tibial plafond, a coronal plane passing through the center of the tibial plafond region was determined. On this plane, we identified a line connecting the most medial and most lateral points of the tibial plafond. Second, this line was divided equally into four segments by five points (medial point, medial 1/4 point, midpoint, lateral 1/4 point, lateral point) (*Figure 3*). Third, five sagittal sections were determined passing the above five points. Lastly, on each sagittal section, five points (Anterior point, Posterior point, Top point, Anterior midpoint and Posterior midpoint) were

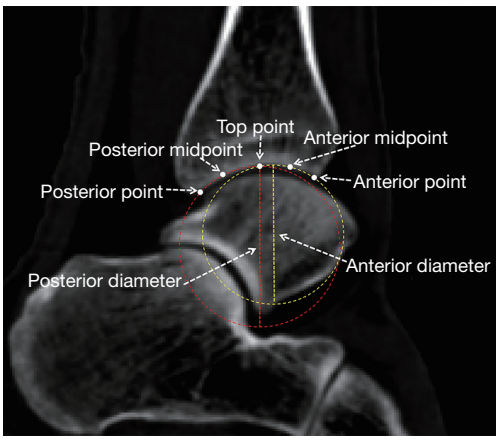

Figure 4 Measurements of the anterior and posterior diameters of the tibial plafond.

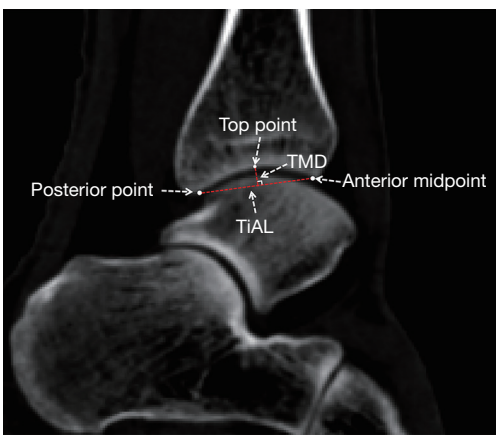

Figure 5 Measurements of the TiAL and TMD. TiAL, distal tibial arc length; TMD, distal tibial mortise depth.

determined. The anterior, posterior and top points were defined as the most anterior, posterior and top points of the sagittal arc of tibial plafond, respectively. The anterior midpoint was defined as follows: (I) drawing the line connecting the anterior point and top point; (II) drawing a line perpendicular to this line and passing this midpoint of this line; (III) determining the anterior midpoint as the intersection point of this line and the sagittal arc line of tibial plafond. The posterior midpoint was determined as the similar steps (*Figure 4*). The diameter of the tibial plafond was automatically calculated by Mimics software. TiAL was measured by connecting the anterior and posterior points of the arc of the sagittal sections of tibial plafond, and TMD was measured as the perpendicular line from the top point of tibial arc to distal tibial arc line (*Figure 5*).

All measurements were performed twice by one orthopedic surgeon independently with an interval of 8 weeks to assess the intraobserver measurement reproducibility, and the average value was used for statistical analysis. Another author (K.Z.) also performed measurements to assess the interobserver reproducibility. The intraobserver and interobserver reproducibility of measurements was assessed by intraclass correlation coefficients (ICCs): an ICC less than 0.40 indicated poor reliability; an ICC between 0.40 and 0.75 indicated fair to good reliability; an ICC greater than 0.75 indicated excellent reliability. For the outcomes in our study, the ICCs ranged from 0.81 to 0.94, indicating excellent intraindividual and interobserver agreements.

Statistical analysis

The sample size for this study was calculated using the software of G*Power 3.1.9 (Heinrich Heine University Düsseldorf, Germany) based on preliminary data from 40 patients. The minimum number of patients was 90 to achieve a power of 0.95 (effect size =0.7; α=0.05), so we included 100 ankles to ensure a sufficient sample size. During data collection, we used unit standardization and decimal place normalization in this study. The normal distribution of data was examined by Kolmogorov-Smirnov test. Mean values with standard deviations and median with interquartile ranges were calculated for normally and non-normally distributed variables, respectively. The paired *t*-test was used to examine the differences between the anterior and posterior diameters of the tibial plafond. To minimize the effect of height on the results, the normalized data through dividing the original data by height were compared for the subgroup analysis between males and females. For data with normal distribution, independent samples *t*-test was used for a subgroup analysis. For data with non-normal distribution, Mann-Whitney U Test was used as the non-parametric analysis method. One-way analysis of variance (ANOVA) was used to compare the differences among three or more groups. All analyses were performed with SPSS software (version 22.0, SPSS Inc., USA). P values less than 0.05 were considered statistically significant.

Results

This study included 100 healthy ankles from 100 individuals (50 males and 50 females). The non-normally distributed

variables included age, height and weight (P<0.05). The mean age was 23.5±3.7 years; height was 166.6±13.5 cm; BMI was 22.0±3.7 kg/m^2. Patient demographics are shown in *Table 1*.

The outcomes of anterior and posterior diameters of tibial plafond

The diameters of tibial plafond are summarized in *Table 2*. The non-normally distributed variables included the mid-anterior and posterolateral 1/4 diameter of tibial plafond (P<0.05). Analysis of the sagittal curvature on five sagittal sections showed that the anterior diameter of tibial plafond was significantly smaller than the posterior diameter with a mean difference ranging from 3.9 to 6.8 mm (P<0.001). For the outcomes of anterior diameters, the anteromedial curvature had the smallest diameter (35.3±5.3 mm), and the anterolateral curvature had the largest diameter (38.0±5.8 mm). ANOVA analysis revealed that there were significant differences among five outcomes (F=3.25, P<0.012). Significant differences were found between the anteromedial and the anterolateral diameters (P<0.05), but no differences were found in comparisons between the other two groups.

For the outcomes of the posterior diameter, the posteromedial curvature had the smallest diameter (39.2±6.4 mm), and the posterolateral 1/4 curvature had the largest diameter (median, 43.2 mm). ANOVA analysis revealed significant differences among five groups (F=6.36, P<0.001). Significant differences were found between the posteromedial and the posterolateral diameter (P<0.05), but there were no differences between other two groups.

Table 1 Patient demographic data

Parameters	Outcomes
Number	100
Side (right/left)	50/50
Sex (male/female)	50/50
Age (years)	23.0 (20.3–26.0)
Height (cm)	167.0 (160.3–173.8)
Weight (kg)	62.2±12.8
BMI (kg/m^2)	21.2 (19.5–24.0)

Date are presented as n or mean ± standard deviations or median (interquartile ranges). BMI, body mass index.

The outcomes of TiAL and TMD

The mean values of TiAL varied from 23.4 to 26.3 mm, and TMD varied from 3.4 to 4.2 mm. ANOVA analysis showed that there were significant differences for TiAL and TMD among five groups (F=34.79, P<0.001; F=24.16, P<0.001, respectively) (*Table 2*).

Subgroup analysis of the gender

Subgroup analysis of the normalized data showed that both the anterior diameters and posterior diameters were significantly larger in males than in females (P<0.05) except for the anteromedial (P=0.46), posteromedial (P=0.13), anteromedial 1/4 (P=0.09) and anterolateral 1/4 (P=0.37) diameters (*Table 3*). Moreover, gender also significantly affected the outcomes of TiAL (*Table 4*) and TMD (*Table 5*).

Table 2 Outcomes of the sagittal curvature measurements of tibial plafond

Parameter	Anterior diameter (mm)*	Posterior diameter (mm)*	MD or Z value#	P value#	TiAL (mm)*	TMD (mm)*
The medial section	35.3±5.3	39.2±6.4	–3.9	<0.001	23.4±2.5	3.4±0.6
The medial 1/4 section	36.9±4.7	42.1±5.9	–5.1	<0.001	24.8±2.4	3.6±0.5
The middle section	35.9 (32.7–40.5)	42.9±6.9	–6.4	<0.001	25.5±2.8	3.9±0.5
The lateral 1/4 section	36.7±4.7	43.2 (38.5–47.0)	–7.3	<0.001	26.5±2.6	4.2±0.6
The lateral section	38.0±5.8	42.5±6.7	–4.5	<0.001	26.3±2.5	4.1±0.6
ANOVA analysis	F=3.25, P<0.012	F=6.36, P<0.001	–	–	F=34.79, P<0.001	F=24.16, P<0.001

*, outcomes were presented as mean ± standard deviations for normally distributed data, and median and interquartile ranges for non-normally distributed data; #, outcomes from the comparison between anterior and posterior diameters; MD for the outcomes of the paired *t*-test and Z value for Mann-Whitney U test. mm, millimeter; MD, mean difference; TiAL, distal tibial arc length; TMD, distal tibial mortise depth; ANOVA, analysis of variance.

Table 3 Subgroup analysis of the normalized data for the diameters of tibial plafond

Parameter	Male (n=50) (mm)*	Female (n=50) (mm)*	Z value	P value
The anteromedial diameter	20.9±3.3	21.1 (19, 23.1)	−0.7	0.457
The posteromedial diameter	24.1±4.2	22.6 (20.2, 25)	−1.5	0.133
The anteromedial 1/4 diameter	22.5±5.4	21.7 (19.7, 23.3)	−1.7	0.085
The posteromedial 1/4 diameter	26.1±3.0	23.9 (22.2, 25.7)	−3.5	0.000
The mid-anterior diameter	22.9±3.5	21.1 (19.4, 23.2)	−2.2	0.030
The mid-posterior diameter	26.8 (24.5, 28.2)	24.2 (22.2, 26.2)	−3.5	0.001
The anterolateral 1/4 diameter	22.3±4.2	21.8 (19.9, 23.5)	−0.9	0.366
The posterolateral 1/4 diameter	26.5 (23.8, 28.8)	25 (22.3, 27.5)	−1.8	0.007
The anterolateral diameter	23.1±5.6	22.3 (20, 23.2)	−2.0	0.045
The posterolateral diameter	25.4±4.2	23.6 (22.4, 26.6)	−2.2	0.025

*, outcomes were presented as mean ± standard deviations for normally distributed data, and median and interquartile ranges for non-normally distributed data. mm, millimeter.

Table 4 Subgroup analysis of the normalized data for TiAL

Parameter (TiAL)	Male (n=50) (mm)*	Female (n=50) (mm)*	Z value	P value
The medial section	14.3±1.2	13.9 (12.5, 14.6)	−2.1	0.033
The medial 1/4 section	15.3±3.5	14.3 (13.7, 15.1)	−4.1	0.000
The middle section	15.5±4.2	14.6 (13.9, 15.4)	−4.5	0.000
The lateral 1/4 section	16.1±4.2	15.2 (14.4, 15.8)	−4.7	0.000
The lateral section	16.2±1.1	15.2 (14.1, 16)	−3.9	0.000

*, outcomes were presented as mean ± standard deviations for normally distributed data, and median and interquartile ranges for non-normally distributed data. TiAL, distal tibial arc length; mm, millimeter.

Table 5 Subgroup analysis of the normalized data for TMD

Parameter (TMD)	Male (n=50) (mm)*	Female (n=50) (mm)*	Z value	P value
The medial section	2.1±0.3	1.9 (1.7, 2.1)	−1.9	0.055
The medial 1/4 section	2.2±0.5	2.2 (2.0, 2.3)	−1.8	0.067
The middle section	2.5±0.3	2.2 (2.0, 2.4)	−3.3	0.001
The lateral 1/4 section	2.6 (2.4, 2.9)	2.4 (2.2, 2.6)	−3.0	0.002
The lateral section	2.5±0.4	2.4 (2.2, 2.6)	−1.7	0.099

*, outcomes were presented as mean ± standard deviations for normally distributed data, and median and interquartile ranges for non-normally distributed data. TMD, distal tibial mortise depth; mm, millimeter.

Discussion

The principal findings were that the anterior diameter of tibial plafond was significantly smaller than the posterior diameter, and the anterior and posterior diameters on the most lateral sagittal section were significantly larger than those on the most medial sagittal section. However, the trend of change of the anterior diameter was not consistent with the posterior diameter from the medial to lateral tibial plafond. In addition, we found that gender was an important

factor influencing the sagittal curvatures. Our study provides valuable insights into the sagittal curvatures of the tibial plafond and may serve as an important reference for prosthesis design and sizing.

Most studies usually use cadavers to investigate the ankle morphology (15-17). However, it is difficult to obtain a sufficient sample size for cadavers (18). Compared with cadavers, CT images are a reliable alternative that provide more detailed 3D information on the bony morphometry with a high resolution (4,14,19). To date, several studies have used CT images to investigate the morphology of the ankle joint (2,3,14,18,20). However, most studies define the ankle geometry as a single circle on the sagittal plane (3,14,18). Recently, a bi-radial technique has been introduced to assess the geometry of the ankle joint. Clinically, detailed and comprehensive anatomical descriptions are essential to improve biomechanical understanding and implant design. Therefore, this study was designed to provide a more accurate characterization of the sagittal curvatures of the tibial plafond by dividing it into anterior and posterior regions on multiple sagittal planes.

Previous studies showed that the sagittal geometry of the distal tibia can be regarded as a simple truncated cone (1,6,9). However, our study revealed that the anterior diameter of tibial plafond was significantly smaller than the posterior diameter, and the mean difference ranged from 3.9 to 6.8 mm. This implies that the shape of the tibial plafond might be composed of two irregular cones with different apex on the anterior and posterior cones. From the view of the functional morphology concept, the smaller anterior diameter would produce the anterior and posterior translation during the ankle motion (12). Additionally, we found that the anteromedial curvature had the smallest diameter, and the posterolateral 1/4 curvature had the largest diameter. The complex structure of the tibial plafond would induce irregular six-freedom slipping during ankle dorsiflexion and plantarflexion (12,13). Our results are in agreement with Anderle *et al.* (13). They defined the sagittal geometry of the distal tibia using a bi-radial approach, and found that the anterior radius of the distal tibia was smaller than the posterior radius on the lateral side, but no difference was found on the medial side. Our finding was very essential for better understanding the motion of the joint. However, we could not present the motion regularity of the ankle joint from this anatomical study. More future studies are needed to investigate the effect of the tibial plafond anatomy on the ankle kinematics.

The data are also essential for the implant design as the most prostheses of ankle arthroplasty are designed with a single radius (21). The rationale for the single-radius design of total ankle arthroplasty systems is based on the general hypothesis that the shape of the distal tibia can be similarly described as a simple cylinder with a single diameter (21,22). Wiewiorski *et al.* (7) applied a best-fit method with a single radius circle to examine the talar radii. They found no differences between the medial, midsagittal and lateral side, thus indicating that a cylindrical talar dome. However, our study found significant differences between the anterior and posterior diameters. In addition, no symmetry was found between the medial and lateral diameters, but an increasing trend was found from medial to lateral on sagittal sections. This result could be mirrored in the design of the tibial component, in order to restore the natural kinematics of ankle joint. Moreover, understanding the differences in medial and lateral radii can enable the prosthesis to more accurately match the natural anatomy, which can also minimize wear and friction (18,21). This is important for the longevity of the ankle joint prostheses. Our findings align with the design philosophy of the trabecular metal total ankle instrument system (Zimmer Biomet, USA), which made its lateral sagittal radius larger than the medial radius. Therefore, the future design of ankle arthroplasty systems may focus on the differences between the anterior and posterior diameters in the medial or lateral sagittal geometry, in order to better match the anatomical differences and achieve improved kinematics.

In the subgroup analysis of gender, we utilized a normalization method by dividing the original data by height to minimize the influence of height on the outcomes. Our subgroup analysis revealed that many outcomes of the normalized data indicated that males had larger values for both the anterior and posterior diameters of the sagittal curvatures. However, this trend was not observed in terms of the anteromedial, posteromedial, anteromedial 1/4 and anterolateral 1/4 diameters. The possible explanation for these findings is that gender is not the sole determinant that influences the outcomes, and height or other factors might also play a significant role in the sagittal curvatures of tibial plafond. In addition, the subgroup analysis of gender also showed that gender was an essential factor affecting the outcomes of TiAL and TMD. Awareness of the gender differences in the anatomical morphology contributes to improve the implant designs for ankle arthroplasty. Clinically, if the prosthesis is oversized, the overhang may lead to painful impingement. In contrast, if the prosthesis is too small, more bone will be cut, which interrupts

the blood supply to the talus and leads to talar avascular necrosis. Currently, many studies have shown gender-related differences in the knee joints, and manufacturers have designed the gender-specific implants for total knee arthroplasty to achieve an optimal anatomical fit (23,24). However, few studies have introduced the gender-specific prosthesis for the joint ankle. Our data provide important information for prosthesis design for different genders, but the clinical benefits of gender-specific prosthesis still need to be verified.

Strengths and limitations

The strengths of this study included, first, we used an anatomical coordinate system based on previous studies (10-12), which ensured the standard measurements for sagittal curvatures of the ankle joint (10,11,14,15). Second, to the best of our knowledge, this is the first study to investigate the detailed anatomical morphology of the tibial plafond on five sagittal sections. A more accurate and complete description of the anatomy contributes to a better understanding the kinematics and biomechanics of the ankle joint. Third, our study had a sufficient included population and an equal number of males and females compared with previous studies (1,3-5,13,15). These was essential to minimize the bias from sample size and gender.

Several limitations should also be addressed in this study. First, we only included the Chinese population, which may not be representative of other races globally. Future investigations should include other populations to establish a general data of different races. Second, all 3D models of the ankle joint were based on CT images, which did not show the cartilage layer. Previous studies showed that the thickness of articular cartilage between the anterior and posterior regions of the talar trochlea was less than 0.6 mm, which had little effect on the main results of our study (12,25). Third, this study only included the healthy ankle joint, and further studies may focus on the anatomical differences between the abnormal and the healthy ankle joint. Fourth, although gender differences were found in sagittal curvatures of tibial plafond, more studies are needed to explore the necessity of different implant designs for women and men in similar sizes. Lastly, this was an anatomical study based on CT images, which limited us to perform a more in-depth analysis for the effect of different sagittal curvatures on the ankle functionality. Therefore, further studies are needed to explore the impact of differences between the anterior and posterior radius on the ankle biomechanics and kinematics.

Conclusions

Based on our findings, the sagittal curvatures of the tibial plafond can be described quantitatively using the anterior and posterior diameters on five sagittal sections. Significant differences were found between the anterior and posterior diameters, and gender was an important factor influencing the sagittal curvatures of the tibial plafond. The results of this study provide valuable insight into the sagittal curvatures of the tibial plafond and may serve as an important reference for prosthesis design and sizing. Further biomechanical studies are needed for better understanding the importance of the sagittal curvatures on the ankle joint.

Acknowledgments

Funding: The study was funded by National Natural Science Foundation of China (Nos. 82172378 and 82060413), the Medical Innovation and Development Project of Lanzhou University (No. lzuyxcx-2022-173), and Ministry of Science and Technology of China (No. 2022YFC2009501).

Footnote

Reporting Checklist: The authors have completed the STROBE reporting checklist. Available at https://qims.amegroups.com/article/view/10.21037/qims-23-1807/rc

Conflicts of Interest: All authors have completed the ICMJE uniform disclosure form (available at https://qims.amegroups.com/article/view/10.21037/qims-23-1807/coif). The authors have no conflicts of interest to declare.

Ethical Statement: The authors are accountable for all aspects of the work in ensuring that questions related to the accuracy or integrity of any part of the work are appropriately investigated and resolved. The study was conducted in accordance with the Declaration of Helsinki (as revised in 2013). The Ethics Committee of Lanzhou University Second Hospital approved this study (No. 2022A-556), and the requirement to obtain individual consent for this retrospective analysis was waived.

References

1. Siegler S, Toy J, Seale D, Pedowitz D. The Clinical Biomechanics Award 2013 -- presented by the International Society of Biomechanics: new observations on the morphology of the talar dome and its relationship to ankle kinematics. Clin Biomech (Bristol, Avon) 2014;29:1-6.
2. Tümer N, Arbabi V, Gielis WP, de Jong PA, Weinans H, Tuijthof GJM, Zadpoor AA. Three-dimensional analysis of shape variations and symmetry of the fibula, tibia, calcaneus and talus. J Anat 2019;234:132-44.
3. Kellam PJ, Dekeyser GJ, Rothberg DL, Higgins TF, Haller JM, Marchand LS. Symmetry and reliability of the anterior distal tibial angle and plafond radius of curvature. Injury 2020;51:2309-15.
4. Broos M, Berardo S, Dobbe JGG, Maas M, Streekstra GJ, Wellenberg RHH. Geometric 3D analyses of the foot and ankle using weight-bearing and non weight-bearing cone-beam CT images: The new standard? Eur J Radiol 2021;138:109674.
5. Nozaki S, Watanabe K, Katayose M. Three-dimensional analysis of talar trochlea morphology: Implications for subject-specific kinematics of the talocrural joint. Clin Anat 2016;29:1066-74.
6. Inman VT. The joints of the ankle. Balt: Williams Wilkins, 1976.
7. Wiewiorski M, Hoechel S, Anderson AE, Nowakowski AM, DeOrio JK, Easley ME, Nunley JA, Valderrabano V, Barg A. Computed Tomographic Evaluation of Joint Geometry in Patients With End-Stage Ankle Osteoarthritis. Foot Ankle Int 2016;37:644-51.
8. Islam K, Dobbe A, Komeili A, Duke K, El-Rich M, Dhillon S, Adeeb S, Jomha NM. Symmetry analysis of talus bone: A Geometric morphometric approach. Bone Joint Res 2014;3:139-45.
9. Trovato A, El-Rich M, Adeeb S, Dhillon S, Jomha N. Geometric analysis of the talus and development of a generic talar prosthetic. Foot Ankle Surg 2017;23:89-94.
10. Williams BT, Ahrberg AB, Goldsmith MT, Campbell KJ, Shirley L, Wijdicks CA, LaPrade RF, Clanton TO. Ankle syndesmosis: a qualitative and quantitative anatomic analysis. Am J Sports Med 2015;43:88-97.
11. Wu G, Siegler S, Allard P, Kirtley C, Leardini A, Rosenbaum D, Whittle M, D'Lima DD, Cristofolini L, Witte H, Schmid O, Stokes I; . ISB recommendation on definitions of joint coordinate system of various joints for the reporting of human joint motion--part I: ankle, hip, and spine. International Society of Biomechanics. J Biomech 2002;35:543-8.
12. Nozaki S, Watanabe K, Kato T, Miyakawa T, Kamiya T, Katayose M. Radius of curvature at the talocrural joint surface: inference of subject-specific kinematics. Surg Radiol Anat 2019;41:53-64.
13. Anderle MR, Obert RM, Paxson RD, Brinker LZ, Clancy JT. A bi-radial approach to define the sagittal geometry of the healthy ankle. Foot Ankle Surg 2021;27:813-9.
14. Claassen L, Luedtke P, Yao D, Ettinger S, Daniilidis K, Nowakowski AM, Mueller-Gerbl M, Stukenborg-Colsman C, Plaass C. Ankle morphometry based on computerized tomography. Foot Ankle Surg 2019;25:674-8.
15. Kleipool RP, Vuurberg G, Stufkens SAS, van der Merwe AE, Oostra RJ. Bilateral symmetry of the subtalar joint facets and the relationship between the morphology and osteoarthritic changes. Clin Anat 2020;33:997-1006.
16. Knupp M, Stufkens SA, van Bergen CJ, Blankevoort L, Bolliger L, van Dijk CN, Hintermann B. Effect of supramalleolar varus and valgus deformities on the tibiotalar joint: a cadaveric study. Foot Ankle Int 2011;32:609-15.
17. Stufkens SA, Barg A, Bolliger L, Stucinskas J, Knupp M, Hintermann B. Measurement of the medial distal tibial angle. Foot Ankle Int 2011;32:288-93.
18. Hongyu C, Haowen X, Xiepeng Z, Kehui W, Kailiang C, Yanyan Y, Qing H, Youqiong L, Jincheng W. Three-dimensional morphological analysis and clinical application of ankle joint in Chinese population based on CT reconstruction. Surg Radiol Anat 2020;42:1175-82.
19. Liu Y, Liu W, Chen H, Xie S, Wang C, Liang T, Yu Y, Liu X. Artificial intelligence versus radiologist in the accuracy of fracture detection based on computed tomography images: a multi-dimensional, multi-region analysis. Quant Imaging Med Surg 2023;13:6424-33.
20. Radzi S, Dlaska CE, Cowin G, Robinson M, Pratap J, Schuetz MA, Mishra S, Schmutz B. Can MRI accurately detect pilon articular malreduction? A quantitative comparison between CT and 3T MRI bone models. Quant Imaging Med Surg 2016;6:634-47.

21. Gross CE, Palanca AA, DeOrio JK. Design Rationale for Total Ankle Arthroplasty Systems: An Update. J Am Acad Orthop Surg 2018;26:353-9.
22. Vale C, Almeida JF, Pereira B, Andrade R, Espregueira-Mendes J, Gomes TM, Oliva XM. Complications after total ankle arthroplasty- A systematic review. Foot Ankle Surg 2023;29:32-8.
23. Johnson AJ, Costa CR, Mont MA. Do we need gender-specific total joint arthroplasty? Clin Orthop Relat Res 2011;469:1852-8.
24. Piriou P, Mabit C, Bonnevialle P, Peronne E, Versier G. Are gender-specific femoral implants for total knee arthroplasty necessary? J Arthroplasty 2014;29:742-8.
25. Akiyama K, Sakai T, Sugimoto N, Yoshikawa H, Sugamoto K. Three-dimensional distribution of articular cartilage thickness in the elderly talus and calcaneus analyzing the subchondral bone plate density. Osteoarthritis Cartilage 2012;20:296-304.

Cite this article as: Teng Y, Luo H, Cai Y, Li S, Yu J, Zhang K, Lu F, Chen W, Wang X, Ma X. Quantitative analysis of sagittal curvatures of the tibial plafond by computed tomography. Quant Imaging Med Surg 2024;14(7):4913-4922. doi: 10.21037/qims-23-1807

